

## An Analytical Analysis of Quantum Capacitance in Nano-Scale Single-Wall Carbon Nano Tube Field Effect Transistor (CNTFET)

Ajay Kumar Singh

*Faculty of Engineering and Technology, Multimedia University, Melaka Malaysia.*

Received 14 September 2017; Revised 14 October 2017; Accepted 3 January 2018

### ABSTRACT

*This paper discusses the quantum capacitance effect in single-wall conventional CNTFET devices. The analytical expression for quantum capacitance has been derived based on the normalized number of carriers/total charge density. The total charge density in the inverted channel is suppressed at large drain voltage but remains unaffected by introducing any new sub-band. Lowering the quantum capacitance in the CNTFET device is a major challenge to improve the performance of the device. Quantum capacitance takes lower value at higher sub-band when operated at low gate bias voltage. Lower quantum capacitance can be achieved for larger tube's diameter due to reduced band gap and by controlling the BTBT (band-to-band tunneling) leakage current which is possible by choosing the proper dielectric material and gate oxide thickness.*

**Keywords:** Carbon Nano Tube, Density of States, Gate Capacitance, Quantum Capacitance, Total Charge Density]

### 1. INTRODUCTION

Single-wall carbon nanotube field effect transistor (CNTFET) is future candidate to replace conventional Si-MOSFET due to better control of the short channel effects (SCEs) in nano scale regime [1-4]. CNTs are graphite sheets in the shape of tube and can be classified as metallic or semiconductor depending on the direction in which the nanotubes are rolled (Figure 1(a)) [5-6]. The semiconductor nanotubes are mainly used in the design of high performance transistors where channel is the tube itself (Figure 1(b)) [7-9]. There has been immense research carried out by researchers to understand the electrical behavior of CNTFETs [10-12]. The various capacitances in CNTFET devices are shown in Figure 1(c), where  $C_g$  is total capacitance between channel and gate,  $C_s$  and  $C_d$  are the parasitic capacitances in the channel at the source/drain end respectively [13]. From the circuit's point of view, it is necessary to study capacitance  $C_g$  which is expressed as the series combination of gate oxide capacitance ( $C_{ox}$ ) and inversion layer capacitance ( $C_{inv.}$ ) (Figure 1(d)) [14-15]. The inversion layer capacitance is represented by the series combination of quantum capacitance ( $C_q$ ) and electrostatic capacitance for only one occupied sub-band. Quantum capacitance ( $C_q$ ) is a consequence of Pauli Exclusion Principle which requires an extra energy to fill the quantum well with electrons and was first introduced by S. Luryi [16].  $C_q$  is bias dependent and associated with channel material. For nanometer oxide thickness,  $C_{ox}$  approaches to the inversion capacitor (Figure 1(d)) and hence in this situation quantum capacitance starts to affect the total

capacitance of the device. Effect of quantum capacitance is quite prominent in the case of CNTFET devices due to relatively low density of state (DOS). Researchers have studied the quantum capacitance in CNTFET [17-20] in detail but no proper analytical expression is available in the literature.

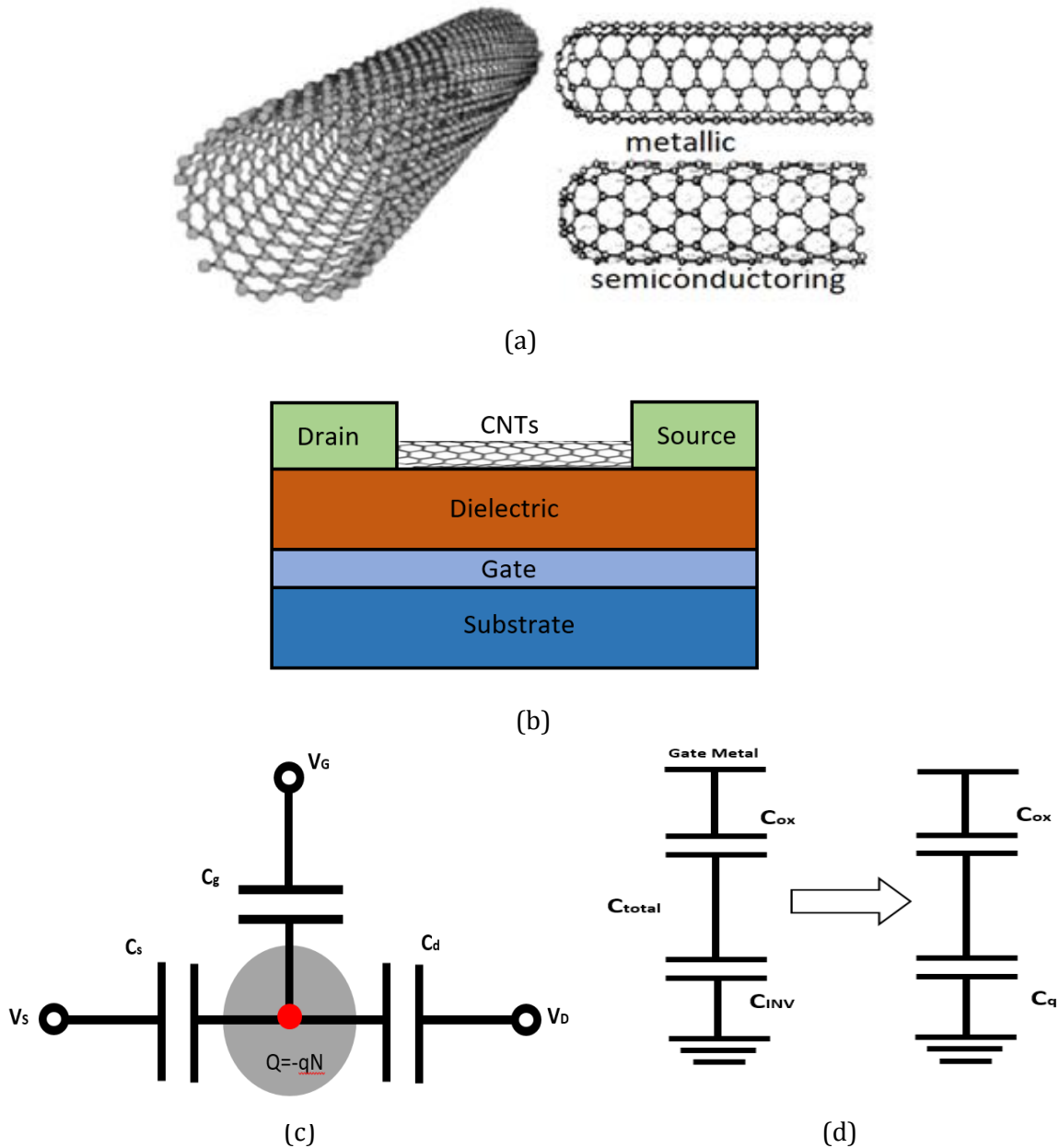


**Figure 1.** (a) Structure and type for CNTs [6] (b) Structure of semiconductor nanotube [7] (c) Various capacitances in CNTFETs [13] (d) Total gate capacitance in CNTFETs [14].

In this present paper, we have analyzed the quantum capacitance in the single-wall CNTFET device after proposing an analytical expression based on carrier charge density. The analytical expression shows that  $C_q$  depends on the bias voltage and oxide/channel material. It has been observed that

the total charge density in the channel is suppressed in the inversion region at large drain voltage whereas it does not show any variation with gate voltage. In subthreshold region,  $C_q$  remains insensitive to the change in drain voltage but decreases with gate voltage due to negligible quantization effect. The performance of the CNTFET devices can be improved by reducing the quantum capacitance which can be achieved by increasing the tube's diameter or choosing the gate material of higher dielectric permittivity. The rest of the paper is organized as follows; section II describes the analytical expressions of total charge density and quantum capacitance. Section III discusses the simulation results and section IV concludes the paper.

## 2. ANALYTICAL MODELS

Quantum capacitance ( $C_q$ ) physically originates from the penetration of the Fermi-level ( $E_F$ ) into conduction band. In carbon nanotube field effect transistor (CNTFET), quantum capacitance needs to be considered because  $C_q$  is comparable to the oxide capacitance ( $C_{ox}$ ) and defined as [18];

$$C_q = \frac{dQ_{cnt}}{dV_a} \quad (1)$$

Where  $V_a$  is applied local potential and  $Q_{cnt}$  is charge density which is given as;

$$Q_{cnt} = q \sum_p n_{CNT} \quad (2)$$

$n_{CNT}$  is the number of carriers in the  $p^{\text{th}}$  sub-band [21];

$$n_{CNT} = \int_0^\infty D_{CNT} \left( \frac{E-E_0}{2} \right) f(E - E_0 - E_{Fi}) dE \quad (3)$$

$E_0$  is mid band gap ( $=qV_{CNT} + \text{deltap}$ ),  $\text{deltap}$  is equilibrium conduction band minima of the  $p^{\text{th}}$  sub-band,  $V_{CNT}$  is modulated potential in the channel due to gate bias voltage,  $D_{CNT}$  is the density of states (DOS) and given as [21];

$$D_{CNT} = \frac{N_0(E - qV_{CNT} + \text{deltap})}{\sqrt{(E - qV_{CNT} + \text{deltap})^2 - (\text{deltap})^2}} \quad (4)$$

$N_0 = \frac{4}{3} \frac{1}{\left(\frac{V_p}{KT}\right)b}$ ,  $V_p$  is carbon-carbon bond energy ( $=3$  eV) and  $b$  is carbon-carbon bond distance ( $=0.142$  nm) and  $f(E - E_0 - E_{Fi})$  is Fermi-Dirac statistics.

The charge at the top of the barriers is controlled from source as well as drain. All the  $+k$ -states at the bottom of the top is occupied by source while  $-k$  states are filled by the drain and hence equation (3) is rewritten as;

$$n_{CNT} = \left( \frac{N_0}{2} \right) \left[ \int_0^\infty \frac{(E - qV_{CNT} + \text{deltap})}{\sqrt{(E - qV_{CNT} + \text{deltap})^2 - (\text{deltap})^2}} \left\{ \frac{1}{1 + e^{\left(\frac{E - qV_{CNT} + \text{deltap} - E_{Fs}}{KT}\right)}} + \frac{1}{1 + e^{\left(\frac{E - qV_{CNT} + \text{deltap} - E_{Fd}}{KT}\right)}} \right\} dE \right] \quad (5)$$

$E_{Fs}$  ( $E_{Fd}$ ) is the source (drain) Fermi-Level. After assuming,  $E_{Fs} = qv_{gs}$  and  $E_{Fd} = qv_{ds}$ , equation (5) can be written as;

$$n_{CNT} = \left( \frac{N_0}{2} \right) \left[ \int_0^\infty \frac{(E - qV_{CNT} + \text{deltap})}{\sqrt{(E - qV_{CNT} + \text{deltap})^2 - (\Delta p)^2}} \left\{ \frac{1}{1 + e^{\left(\frac{E - qV_{CNT} + \text{deltap} - qv_{gs}}{KT}\right)}} + \frac{1}{1 + e^{\left(\frac{E - qV_{CNT} + \text{deltap} + qv_{ds}}{KT}\right)}} \right\} dE \right] \quad (6)$$

Expressing the gate-source and drain-source voltages in terms of applied voltage  $V_a$  as;  $V_a = v_{ds} - V_{CNT}$  at the drain end and  $V_a = v_{gs} + V_{CNT}$  at the source end, and assuming  $(\frac{E + \text{deltap} \pm qV_a}{KT}) \gg 1$ , equation (6) reduces to;

$$n_{CNT} = \left(\frac{N_0}{2}\right) \cosh\left(\frac{V_a}{V_t}\right) \left[ \int_0^\infty \frac{1}{\sqrt{(1 - (\frac{\text{deltap}}{E - qV_{CNT} - \text{deltap}})^2)}} \left\{ e^{-\left(\frac{E + \text{deltap}}{KT}\right)} \right\} dE \right] \quad (7)$$

After performing the integration, we get;

$$n_{CNT} = \left(\frac{N_0}{2}\right) \cosh\left(\frac{V_a}{V_t}\right) e^{-\left(\frac{V_{CNT}}{V_t}\right)} \left[ + \left(\frac{\text{deltap}}{KT\sqrt{2}}\right)^2 \{E_i(\text{beta}) - \left(\frac{1}{\text{beta}}\right) e^{-\text{beta}}\} \right] \quad (8)$$

Where,  $E_i(\text{beta})$  is the exponential integration factor and  $\text{beta} = \frac{qV_{CNT} - \text{deltap}}{KT}$ .

From equation (8), it is observed that the number of carriers in the channel reduces to zero when

$$v_{gs} = \ln \left[ \frac{qn_i}{C_{ox}} \ln \left( 1 + \gamma \frac{v_{ds}}{V_t} \right) \right]$$

Where,  $\gamma$  is fitting parameter and  $n_i$  is intrinsic carrier concentration. Using equation (8), the total charge density in the channel is given as;

$$Q_{cnt} = q \left(\frac{N_0}{2}\right) \cosh\left(\frac{V_a}{V_t}\right) \exp\left(-\frac{V_{CNT}}{V_t}\right) \left[ e^{\text{beta}} + \left(\frac{\text{deltap}}{KT\sqrt{2}}\right)^2 \{E_i(\text{beta}) - \left(\frac{1}{\text{beta}}\right) e^{-\text{beta}}\} \right] \quad (9)$$

And hence finally expression for quantum capacitance in the single-wall CNTFET device is given as;

$$C_q = q \left(\frac{N_0}{V_t}\right) \sinh\left(\frac{V_a}{V_t}\right) e^{-\left(\frac{V_{CNT}}{V_t}\right)} \left[ \left(1 + \coth\left(\frac{V_a}{V_t}\right)\right) \left\{ e^{\text{beta}} + \left(\frac{\text{deltap}}{KT\sqrt{2}}\right)^2 \left( E_i(\text{beta}) - \left(\frac{1}{\text{beta}}\right) e^{-\text{beta}} \right) - \coth\left(\frac{V_a}{V_t}\right) \left\{ e^{\text{beta}} + \left(\frac{\text{deltap}}{KT\sqrt{2}}\right)^2 \left( \frac{\cosh(\text{beta})}{2\text{beta}} - \left(\frac{1}{\text{beta}}\right)^2 e^{-\text{beta}} \right) \right\} \right] \quad (10)$$

Equation (10) shows that  $C_q$  is bias dependent [22] and proportional to the density of states (DOS). It is also observed that as  $V_a \rightarrow 0$ ,  $C_q$  reduces to zero (quantum capacitance limit). In the quantum capacitance limit, instead of holding the charge constant the gate holds the nanotube potential constant at the gate. We have also observed that for  $qV_{CNT} = \text{deltap}$ , quantum capacitance approaches to its classical limit ( $C_q \rightarrow \infty$ ).

Now let us consider two cases;

**Case1:** when "beta" is negative. Equation (8) reduces to;

$$n_{CNT} \cong A e^{-\text{beta}} \quad (11)$$

Where,  $A = \cosh\left(\frac{V_a}{V_t}\right) e^{-\left(\frac{V_{CNT}}{V_t}\right)}$ .

This expression predicts that the number of normalized carrier density falls exponentially for negative beta.

**Case 2:** When “beta” is positive. The normalized carrier density reduces to;

$$(n_{CNT})/N_0 \cong B + C * \text{beta} \tag{12}$$

$$B = \cosh\left(\frac{Va}{V_t}\right) e^{-\left(\frac{\text{deltap}}{KT}\right)} \left[\left(\frac{3}{2} - \frac{2V_{CNT}}{V_t}\right)\right]$$

And

$$C = \left(\frac{1}{2}\right) \cosh\left(\frac{Va}{V_t}\right) e^{-\left(\frac{\text{deltap}}{KT}\right)}$$

Expression 12 shows that the number of carriers increases linearly for positive beta.

**Case 3:** For continuity at beta=0, it is required that A=B and hence the necessary condition for continuity is;

$$\left(\frac{vgs - Va}{V_t}\right) = \left(\frac{1}{2}\right)$$

### 3. SIMULATION RESULTS AND DISCUSSION

Following values of various parameters have been chosen for the simulation of single-wall CNTFET device; tox (oxide thickness) = 10 nm, rcnt (radius of the tube) = 1 nm, L= 10 nm, vds= 0.05 V, vgs= 0.2 V.

The lower value of drain voltage is purposely chosen so that gate has effective control of the channel over the external field. The number of carriers in the channel increases linearly with gate bias voltage due to decrease in source-channel barrier height at large gate voltage. At higher gate voltage it is observed that carrier remain insensitive towards temperature change due to access resistance limitation in CNTFET. The charge carrier density in the tube is suppressed appreciably in inversion region compared to the subthreshold region at higher drain voltage irrespective of the gate voltage.

Figures 2(a) and 2(b) respectively validate our findings that for positive beta, the normalized carrier density increases linearly whereas it falls exponentially for negative beta.

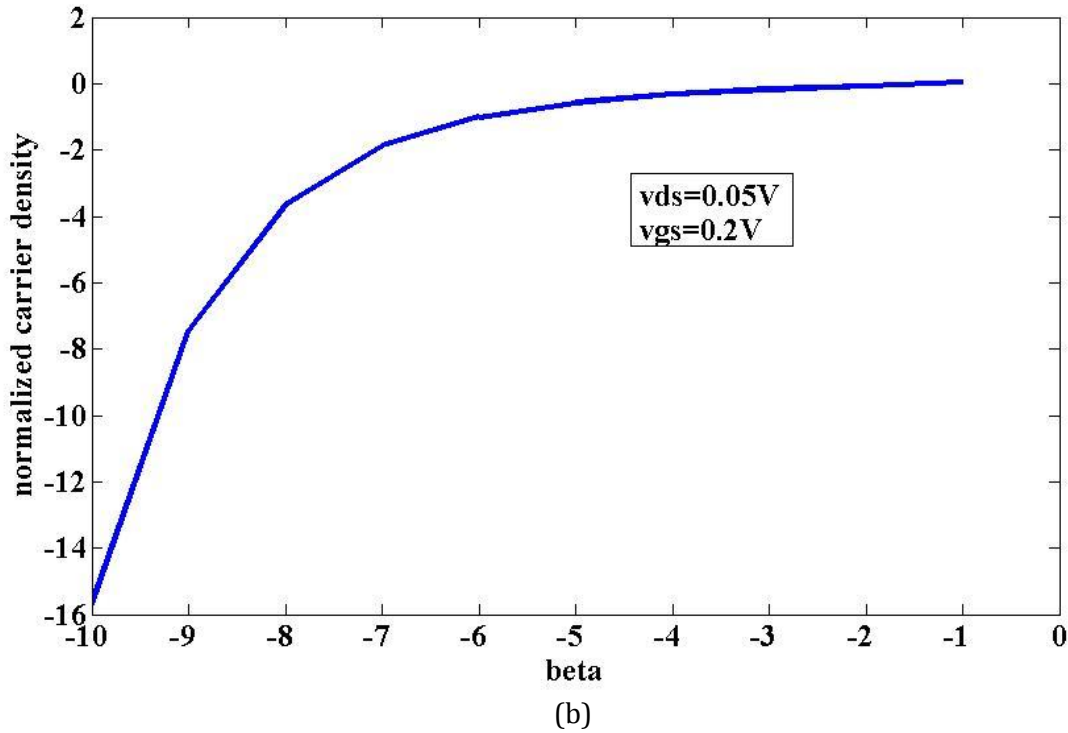
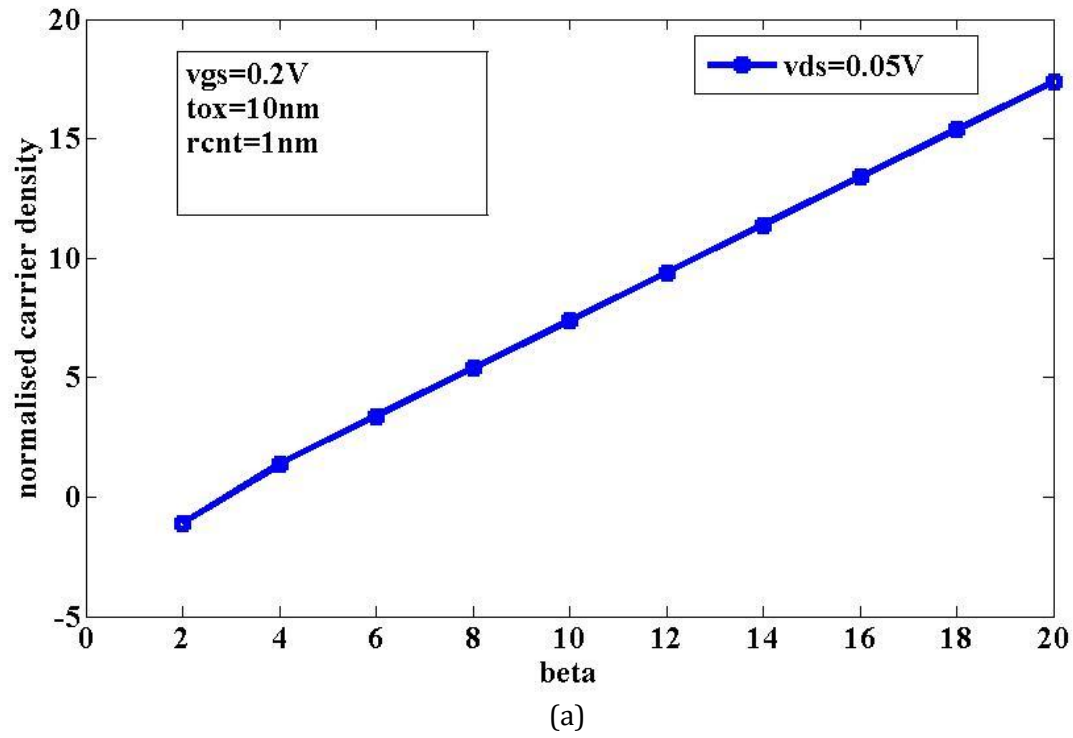


Figure 2. Variation of normalized carrier density (a) for positive beta (b) negative beta.

The developed expression (8) was validated with excellent agreement with ref. [23] models as shown in Figure 3.

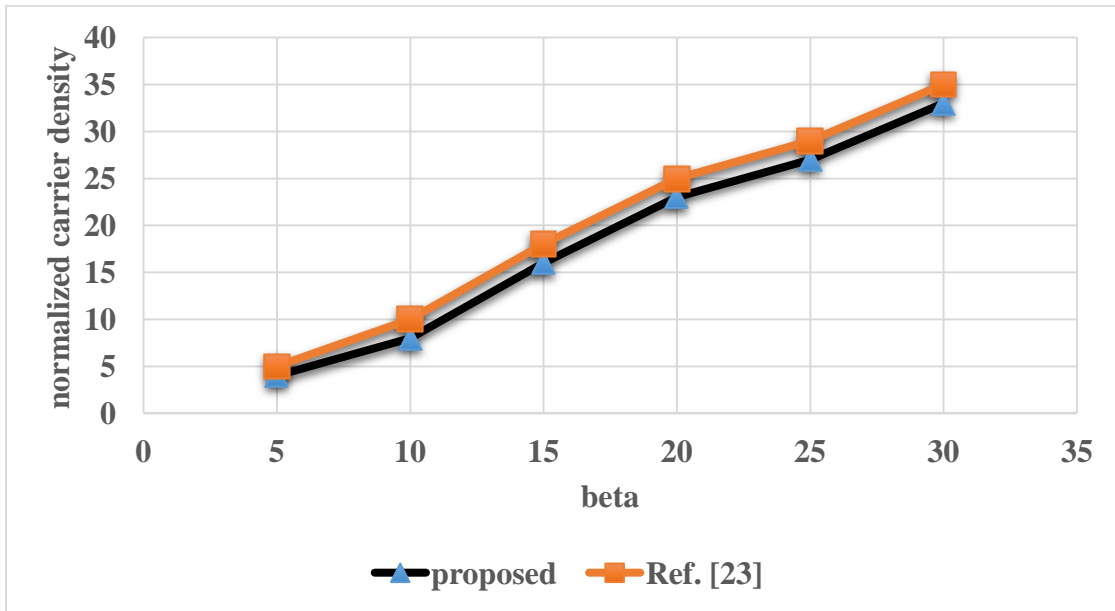


Figure 3. Comparison of normalized carrier density with equation (8) and ref [23].

Figure 4 shows the variation of normalized  $\log Q_{CNT}$  with applied voltage  $V_a$  for different  $\delta$ . The charge carrier density is normalized with respect to  $N_0$ . It is observed that the number of carriers is larger in the lower sub-band compared to the higher sub-band due to lower energy required to move the carriers from the valence band to conduction band. Generally, carrier density increases with bias voltage due to increased conduction in inversion region of the device.

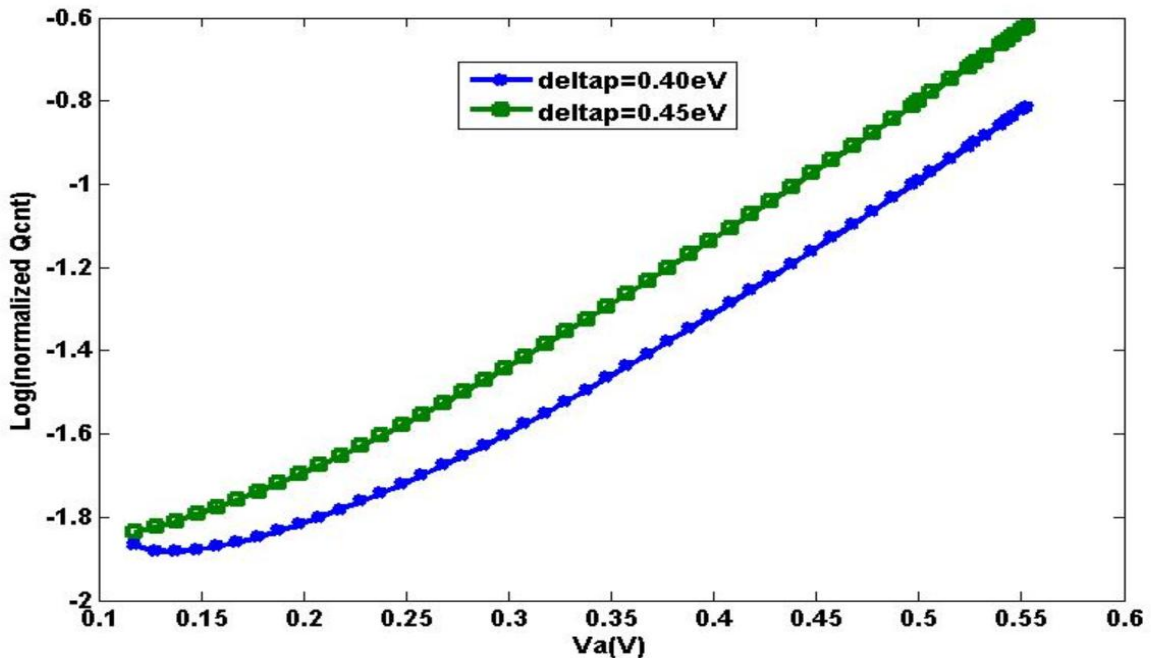


Figure 4. Variation of normalized  $Q_{CNT}$  against  $V_a$  for two sub-bands.

The charge density  $Q_{cnt}$  decreases as drain bias voltage ( $v_{ds}$ ) increases because the increased drain voltage suppresses the  $-k$  half of the distribution function which reduces the charge density irrespective of sub-band value (Figure 5).

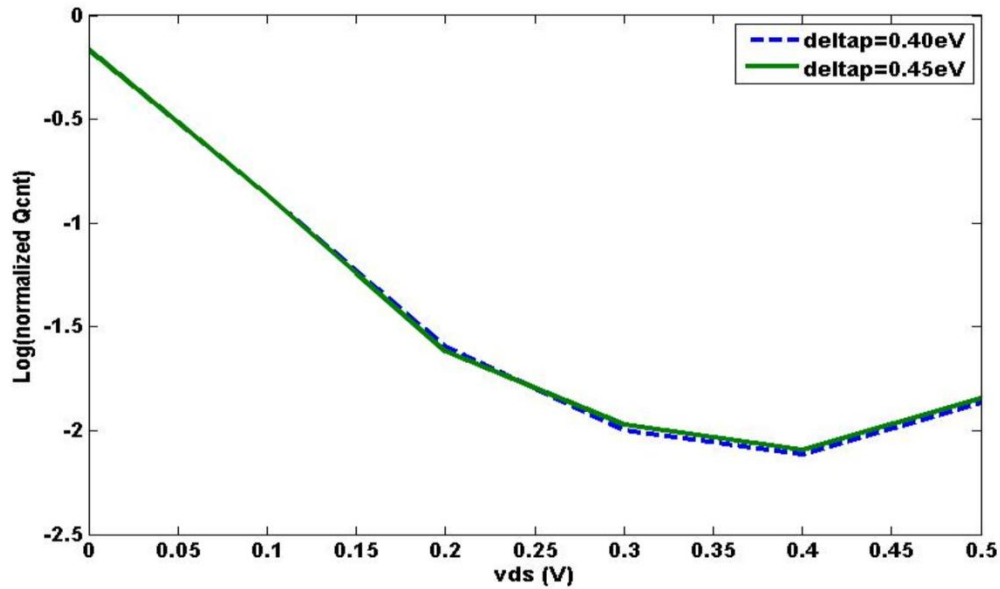


Figure 5. Normalized  $Q_{CNT}$  variation with  $v_{ds}$  for two sub-bands.

Charge density  $Q_{cnt}$  increases exponentially with gate voltage ( $v_{gs}$ ) (Figure 6) because nanotube potential is pinned by the gate voltage which results in larger charge density in the channel. An appreciable effect of  $\text{deltap}$  is observed on normalized  $Q_{cnt}$  only at lower gate voltage due to BTBT tunneling effect.

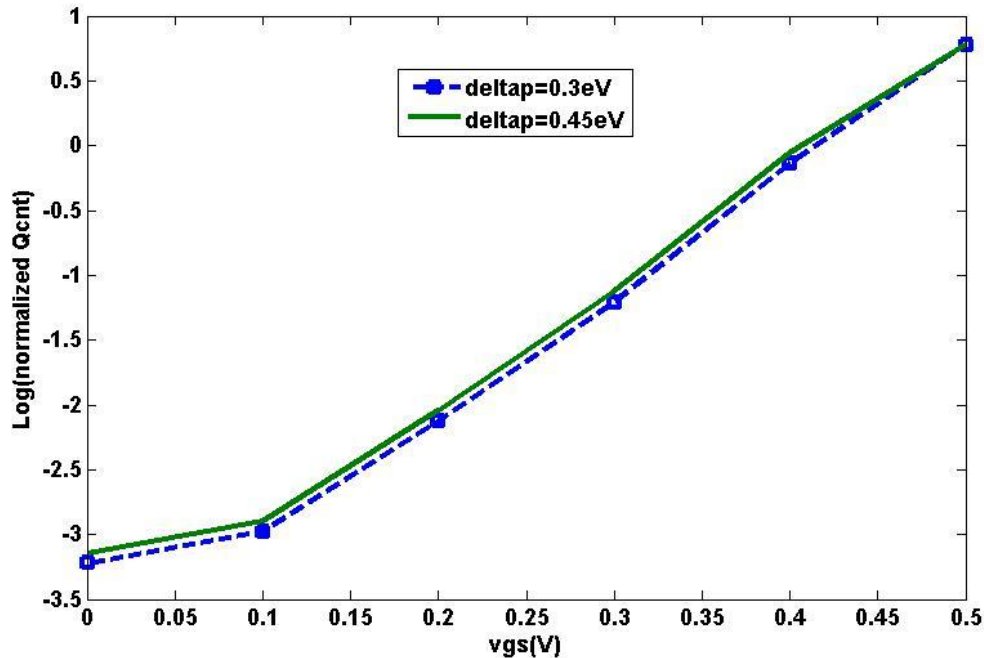


Figure 6. Log ( $Q_{CNT}$ ) versus  $v_{gs}$  for two different values of  $\text{deltap}$ .



To validate the proposed analytical expression (10), we have compared the simulated results of expression (10) with the results provided in ref. [20] for  $t_{ox}=0.7nm$ . The comparison results are given in table 1. The difference between two results is due to negligence of short channel effects in the analytical expression (10).

**Table 1** Comparison of quantum capacitance with ref [20]

vds=0V, d=0.7nm, Kr=1		
vgs (V)	Quantum capacitance (F/m)	
	Calculated using expression (10)	Ref. [20]
0.0	$6.32 \times 10^{-16}$	$5.12 \times 10^{-16}$
0.05	$4.37 \times 10^{-15}$	$3.85 \times 10^{-15}$
0.10	$3.02 \times 10^{-14}$	$2.50 \times 10^{-14}$
0.15	$2.09 \times 10^{-13}$	$2.10 \times 10^{-13}$
0.20	$1.44 \times 10^{-12}$	$1.15 \times 10^{-12}$

The quantum capacitance measures the density of states (DOS) which undergoes a large transition as Fermi level is pushed inside the sub-bands at large gate voltage. At high voltage, upper valleys get populated which allows a continuous increase in  $C_q$  (Figure 7). Since, in CNT the energy gap is inversely proportional to the diameter of the tube, therefore, larger diameter gives lower energy gap which results in lower  $C_q$  as seen from Figure 7. The increase in quantum capacitance with increase in gate bias voltage is more pronounced in inversion region compared to subthreshold region due to dominance of quantum effect in nano-scale device.

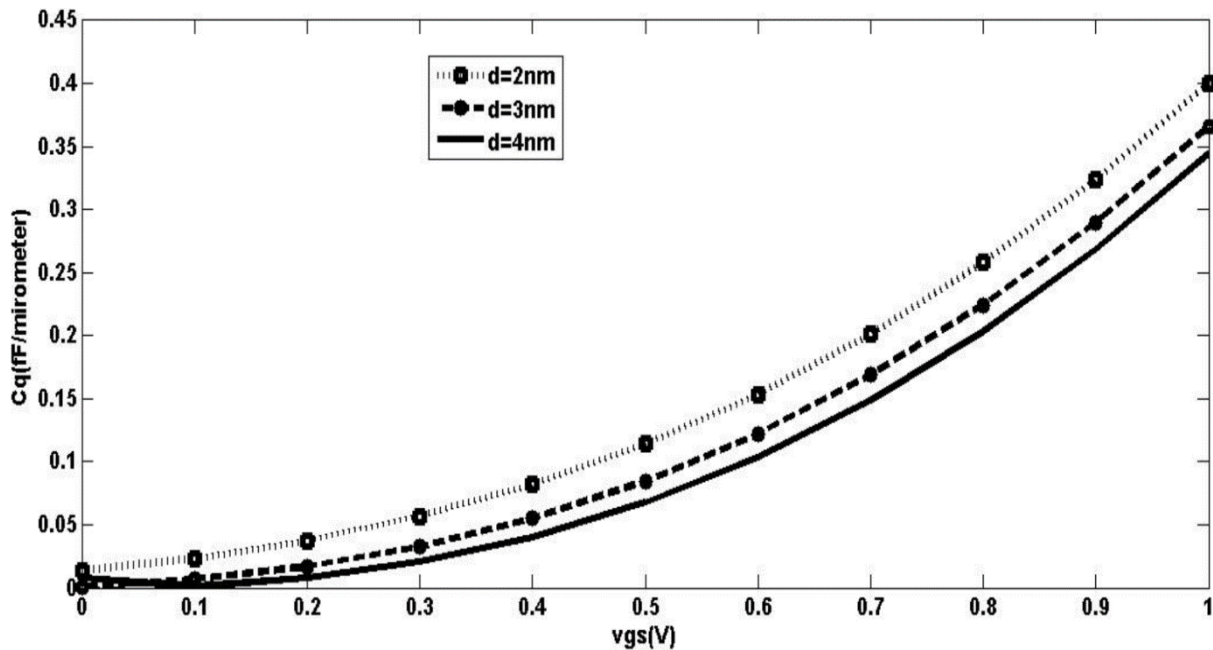


**Figure 7.** Variation of  $C_q$  with  $v_{gs}$  for various tube's diameters (d).

The energy level is smaller in the case of first occupied sub-band than the higher sub-bands. The lower energy gap of the first sub-band results in lower quantum capacitance compared to the second sub-band ( $\text{deltap}=0.9\text{eV}$ ) (Figure 8).

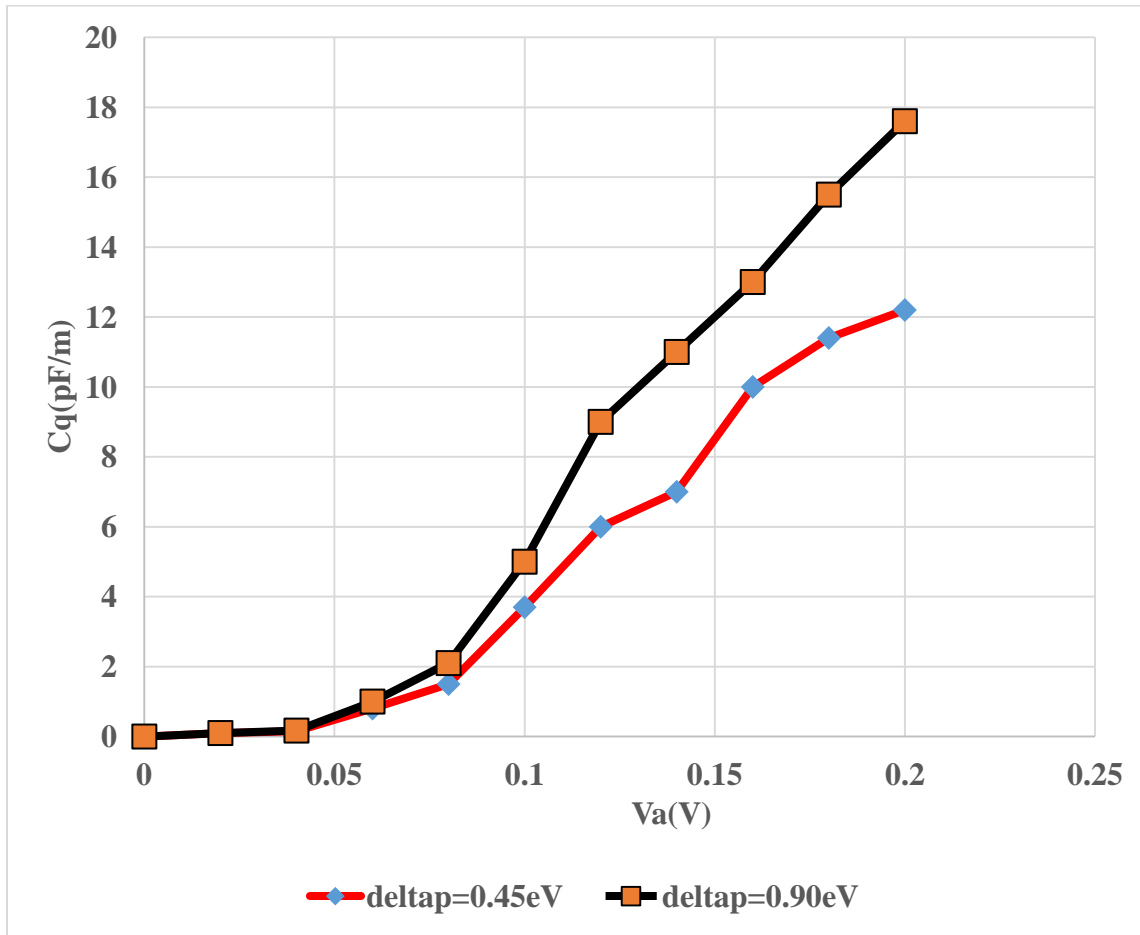


**Figure 8.**  $C_q$  versus  $V_a$  for first and second sub bands.

At higher drain voltage,  $C_q$  takes lower value due to suppressed Fermi level in CNTFET device which results in lower density of states (DOS) as shown in Figure 9. The simulation results also suggest that by raising the drain and gate voltages, the quantum capacitance in CNTFET device can be reduced drastically.

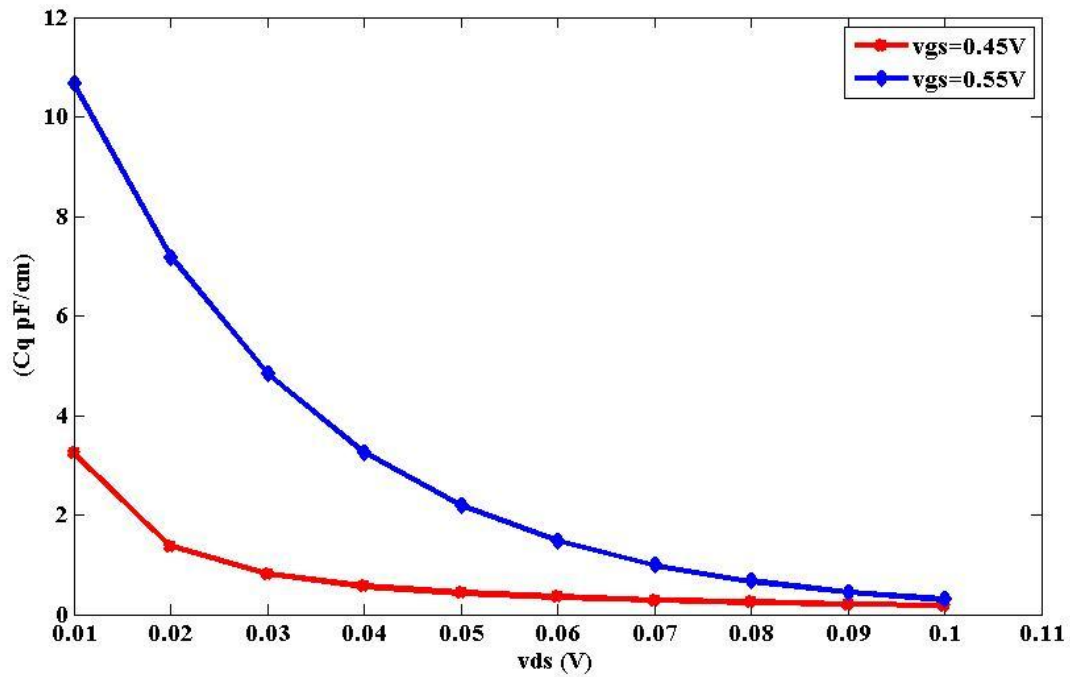


Figure 9. Variation of  $C_q$  with  $v_{ds}$  for two gate bias voltages ( $v_{gs}$ ).

In CNTFET device, high relative dielectric material ( $K_r$ ) can be easily achieved which lowers the quantum capacitance due to better control of tunneling current in the channel as shown in Figure 10.

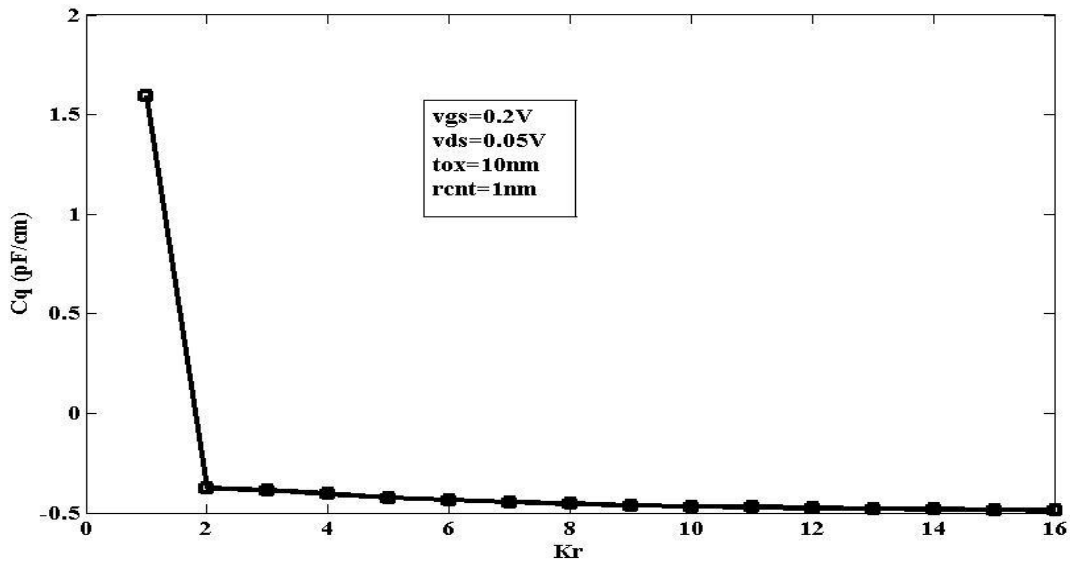
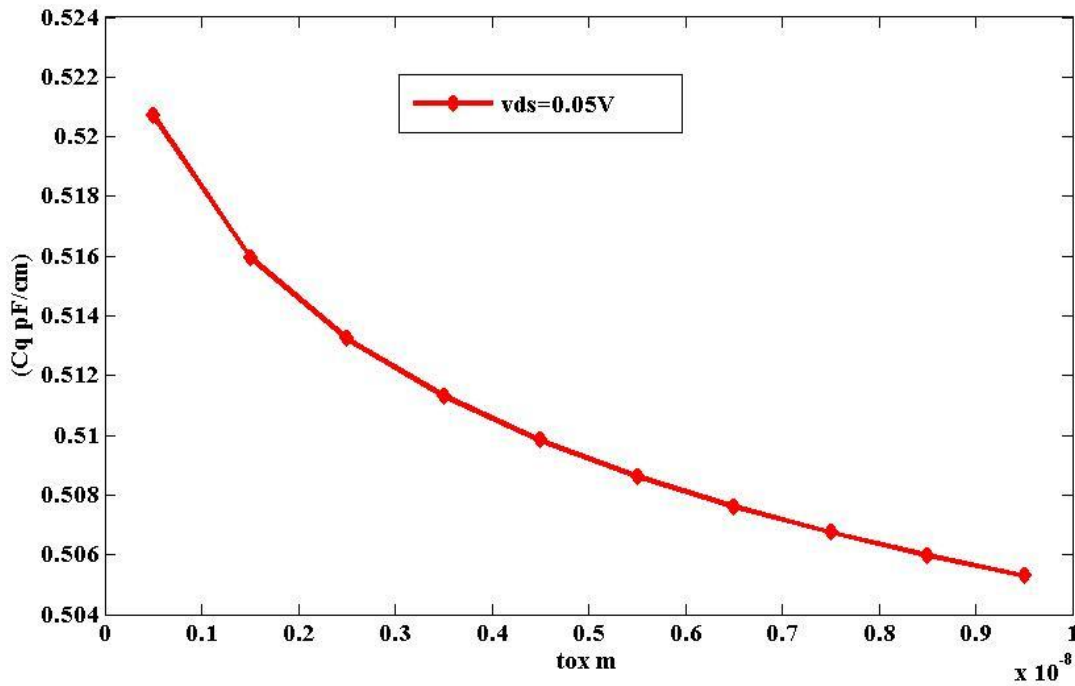


Figure 10. Effect of relative dielectric ( $K_r$ ) constant on  $C_q$ .

$C_q$  reduces for thicker gate oxide ( $t_{ox}$ ) compared to the thinner oxide due to effective control of leakage current in the device irrespective of the applied gate/drain voltages (Figure 11).



**Figure 11.** Effect of oxide thickness ( $t_{ox}$ ) on the  $C_q$ .

It is also observed that when tube of radius 1nm and gate thickness of 0.25 nm is occupied by one sub-band then quantum capacitance value approaches to approximately 4 pF/cm.

#### 4. CONCLUSION

Due to lower density of states in CNTFET devices, the quantum capacitance becomes comparable to oxide capacitance which starts to affect the gate capacitance. In this paper an analytical expression for the quantum capacitance has been proposed. In subthreshold region, due to negligible quantization effect quantum capacitance does not affect the performance of CNTFET device severely compared to the inversion region. In general, quantum capacitance takes lower value for larger oxide thickness and relative permittivity of the gate material. Quantum capacitance also suppressed at higher drain voltage and larger tube's diameter. Lower quantum capacitance results in improved propagation delay and reduced leakage current which improves the performance of the device.

## REFERENCES

- [1] Appenzeller, Y. Lin, J. Knoch, Z. Chen, P. Avouris, "Comparing carbon nanotube transistors—The ideal choice: A novel tunneling device design", *IEEE Trans. Electron Devices* **52**, 12 (2005) 2568-2576.
- [2] A. D. Franklin, "Electronics: The road to carbon nanotube transistors", *Nature* **498**, 7455 (2013) 443-444.
- [3] L.-M. Peng, Z. Zhang, S. Wang, "Carbon nanotube electronics: Recent advances", *Mater. Today* **17**, 9 (2014) 433-442.
- [4] Roberto Marani and Anna Gina Perri, "The next generation of FETs: CNTFETs", *International Journal of Advances in Engineering & Technology (IJAET)* **8**, 5 (2015) 854-866.
- [5] L. Ding et al., "Selective growth of well-aligned semiconducting single-walled carbon nanotubes", *Nano Lett.*, **9**, 2, (2009) 800-805.
- [6] D. Fathi, B. Forouzandeh, "Interconnect challenges and carbon nanotube as interconnect in nano VLSI circuits" in *Carbon Nanotubes, USA, LA, Baton Rouge: InTech*, (2010).
- [7] Q. J. Appenzeller, "Carbon nanotubes for high-performance electronics—Progress and prospect", *Proc. IEEE* **96**, (2008) 201-211.
- [8] G. S. Tulevski, Aaron D. Franklin, David Frank, Jose M. Lobe, Qing Cao, Hongsik Park, Ali Afzali, Shu-Jen Han, James B. Hannon and Wilfried Haensch, "Toward high-performance digital logic technology with carbon nanotubes", *ACS Nano* **8**, 9, (2014) 8730-8745.
- [9] Jun-Young Jeon and Tae-Jun Ha, "High-Performance Single-Walled Carbon Nanotube-Based Thin-Film Transistors by Reducing Charge Transfer", *IEEE Trans. on Electron Devices* **63**, 2 (2016) 827-831
- [10] T. Mizutani, Y. Ohno, S. Kishimoto, "Electrical properties of Carbon nanotube FETs", *International Conference on Advanced Semiconductor Devices and Microsystems, (ASDAM-2008)*, (2008) 1-8.
- [11] A. Fediai, D. A. Ryndyk, G. Seifert, S. Mothes, M. Claus, M. Schröter, G. Cuniberti, "Towards an optimal contact metal for CNTFETs", *Nanoscale* **8**, 19(2016) 10240.
- [12] B. Naresh Kumar, Ajay Kumar Singh, C. M. R. Prabhu, C. Venkateshaiah, and Gan Che Sheng, "Compact Analytical Model for One Dimensional Carbon Nanotube Field Effect Transistor (CNTFET)", *ECS Solid State Letters* **4**, 6 (2015) M12-M14.
- [13] Safayat-Al Imam, Nasheen Kalam and Sharmin Abdhullah, "Temperature Dependence of Carbon Nanotube Field Effect Transistor under Non-Ballistic Conduction Considering Different Dielectric Materials", *Nanoscience and Nanotechnology* **4**, 3 (2014) 52-58
- [14] Zoheir Kordrostami and Mohammad Hossein Sheikhi, "Fundamental Physical Aspects of Carbon Nanotube Transistors," Jose Mauricio Marulanda (Ed.), ISBN: 978-953-307-054-4, Published March 1, 2010, InTech Publication.
- [15] Jieying Luo, Lan Wei, Chi-Shuen Lee, Aaron D. Franklin, Ximeng Guan, Eric Pop, Dimitri A. Antoniadis and H.-S. Philip Wong, "Compact Model for Carbon Nanotube Field-Effect Transistors Including Nonidealities and Calibrated With Experimental Data Down to 9-nm Gate Length", *IEEE Trans. on Electron Devices* **60**, 6 (2013) 1834-1843.
- [16] S. Luryi, "Quantum Capacitance Devices", *Appl. Phys. Lett.*, **52**, 6(1988) 501-503.
- [17] J. Guo, S. Datta, M. Lundstrom, M. Brink, P. McEuen, A. Javey, H. Dai, H. Kim, P. McIntyre, "Assessment of silicon MOS and carbon nanotube FET performance limits using a general theory of ballistic transistors", *IEDM Tech. Dig.*, (2002) 29.3
- [18] D.L. John, L.C. Castro and D.L. Pulfreyb, "Quantum capacitance in nanoscale device modeling", *Journal of Applied Physics* **96**, 9 (2004) 5180-5184.
- [19] S. Ilani, L.A.K. Donev, M. Kindermann and P.L. McEuen, "Measurement of the quantum capacitance of interacting electrons in Carbon nanotubes," *Nature Physics* **2** (2006) 687-691.

- [20] Sanjeet Kumar Sinha and Saurabh Chaudhury, "Impact of Oxide Thickness on Gate Capacitance—A Comprehensive Analysis on MOSFET, Nanowire FET and CNTFET Devices", *IEEE Trans. on Electron Devices* **12**, 6 (2013) 958-964.
- [21] Sébastien Frégonèse, Hugues Cazin d'Honinchtun, Johnny Goguet, Cristell Maneux, Thomas Zimmer, Jean-Philippe Bourgoïn, Philippe Dollfus, and Sylvie Galdin-Retailleau, "Computationally Efficient Physics-Based Compact CNTFET Model for Circuit Design", *IEEE Trans. on Electron Devices*, **55**, 6 (2008) 1317-1326.
- [22] D. Akinwande and H.-S. P. Wong, "Carbon Nanotube and Graphene Device Physics". Cambridge, U.K.: Cambridge Univ. Press, (2011).
- [23] A. Raychowdhury, S. Mukhopadhyay, K. Roy, "A circuit-compatible model of ballistic carbon nanotube field-effect transistors", *IEEE Trans. Comput.-Aided Design Integr. Circuits Syst.* **23**, 10 (2004) 1411-1420.